ACS OMEGA

Open Access

http://pubs.acs.org/journal/acsodf

Article

Synthesis of Tungsten Oxide, Iron Oxide, and Copper-Doped Iron Oxide Nanocomposites and Evaluation of Their Mixing Effects with Cyromazine against *Spodoptera littoralis* (Boisduval)

Sahar E. Eldesouky,* Dalia G. Aseel, Mohamed S. Elnouby, Fatma H. Galal, Ammar AL-Farga, Elsayed E. Hafez, and Hanaa S. Hussein

Cite This: *ACS Omega* 2023, 8, 44867−44879

Read Online

ACCESS | Metrics & More | Article Recommendations

ABSTRACT: Nanotechnology research is emerging as a cutting-edge technology, and nanocomposites have played a significant role in pest control. Therefore, the present study focuses on the synthesis of tungsten oxide (WO_3), iron oxide (magnetic nanoparticle, MNP), and copper-doped iron oxide (MNP-Cu) nanocomposites and explores the different effects of their binary combinations with the insecticide cyromazine against *Spodoptera littoralis*. The synthesized nanoparticles were characterized by transmission electron microscopy, X-ray diffraction, Fourier-transform infrared spectroscopy, and Raman spectroscopy. None of the tested nanomaterials showed any toxicity against the different stages of *S. littoralis*. Larval and pupal durations increased with increasing cyromazine and nanomaterial concentrations. The longest larval and pupal durations were recorded under treatment with the mixture of cyromazine (100 mg/L) + MNP-Cu (500 mg/L); the survival periods were 23.5 and 15.6 days, compared with 10.8 and 7.7 days in the control, respectively. The percentages of pupation and adult emergence were negatively affected by all treatments. Among the 500 mg/L nanomaterial combinations, only cyromazine (25 mg/L) and WO_3 (500 mg/L) resulted in adult emergence (at a rate of 27.3%). Some abnormalities in the *S. littoralis* stages were observed following treatment with the tested materials. The glutathione *S*-transferase and alpha-esterase enzyme activities in *S. littoralis* were significantly increased after treatment with cyromazine, followed by cyromazine/MNP-Cu combinations. The quantitative polymerase chain reaction (Q-PCR) data showed that all treated insects had a higher immune response than the control. Finally, mixes of nanocomposites and cyromazine may be suggested as viable alternatives for *S. littoralis* management.

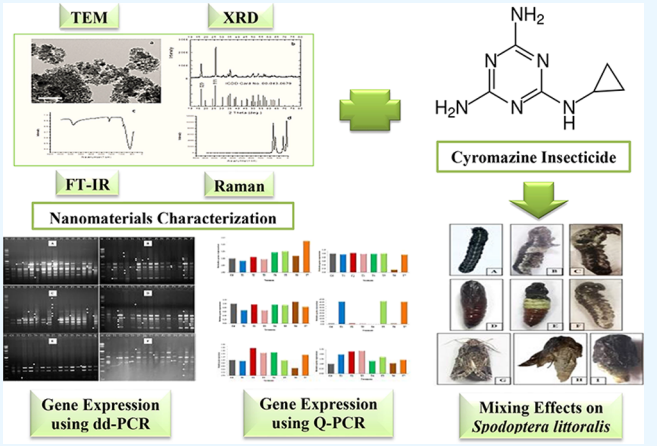

1. INTRODUCTION

The cotton leafworm, *Spodoptera littoralis* (Lepidoptera: Noctuidae), is an important pest in the cotton-growing regions of northern Africa, the Middle East, and the Mediterranean.[1] This pest causes the most damage to more than 180 plant species, including cotton, tomatoes, cabbage, cauliflower, and other crucifers.[2]

Chemical insecticides are the main tools for eradicating *S. littoralis*. The global population uses around 2 million metric tons of pesticides every year. By 2020, 3.5 million tons of pesticides will be used worldwide.[3] Excessive use of traditional pesticides has resulted in numerous problems for the environment,[4,5] including the development of insect resistance to certain insecticides.[6] Researchers have been working hard to produce new effective, environmentally friendly pest control agents to lessen the usage of synthetic pesticides and their harmful impact on the environment.[7,8]

Nanotechnology can be applied to all other science subjects, including chemistry, biology, physics, materials science, engineering,[9] and pest management via successful formulations of nanomaterial-based pesticides.[10,11] Nanoparticles (NPs) with distinct chemical characteristics have the potential for pest control[12,13] and are emerging as a viable alternative to conventional pesticides due to their lower toxicity to humans.[14,15] Possible uses of nanomaterials in agriculture include enhancing plant growth and nutrition, protecting

Received: August 18, 2023
Revised: October 11, 2023
Accepted: October 13, 2023
Published: November 13, 2023

plants from abiotic stress, identifying pathogens, and detecting residues of pesticides.[16]

Recently, magnetic nanomaterials have been used as adsorbents to remove toxic metal ions, pesticides, and antibiotics from polluted wastewater and agricultural wastewater,[17,18] remediate metal-contaminated soils and groundwater,[19,20] promote soil fertility,[21] act as biosensors,[22,23] prime seeds,[24] and deliver treatment to plants.[25,26] Magnetite NPs provide an option that combines both of these characteristics. It is particularly effective at controlling the pest, specifically interfering with its larval development, and it produces little toxicity at the environmental level.[27] The bioapplications based on magnetic NPs have gotten special attention because they have prominent advantages over other materials in terms of cost and ease of manufacture, physical and chemical stability, biocompatibility, and environmental safety, as well as the ability to be tuned and functionalized for specific applications.[28] Metal oxide NPs such as zinc oxide,[29] titanium dioxide,[30] silicon oxide,[31,32] iron oxides,[33,34] copper oxide,[35] and tungsten oxide[36] are also low-cost materials, easy to produce, and chemically stable. As a result, these nanomaterials are excellent candidates for various applications, including water treatment,[37] antimicrobials,[38] sensors, and many more.

Cyromazine (N-cyclopropyl-1,3,5-triazine-2,4,6-triamine) is a very effective insect development disruptor, especially against dipteran insects and a few other insect species, because of its ability to disrupt cuticle production.[39] Cyromazine has been demonstrated to disturb the development of *S. littoralis* and reduce the extensibility of the cuticle.[40,41]

The detoxification enzymes in insects, including glutathione *S*-transferases (GSTs) and α-esterase, are important in their enzymatic defense against exogenous chemicals and in maintaining the insect's regular physiological functions.[42]

The main objectives of this study were to synthesize and characterize inexpensive, biocompatible nanocomposites such as tungsten oxide, iron oxide, and copper-doped iron oxide. This study is the first to investigate the biological, physiological, and biochemical effects of tested nanocomposites as binary combinations with the insecticide cyromazine against *S. littoralis*. In addition, using differential display polymerase chain reaction (dd-PCR) and quantitative polymerase chain reaction (q-PCR), we analyzed the immunological responses of insects to the examined nanomaterials to identify the potential consequences of the compounds tested on this harmful pest.

2. MATERIALS AND METHODS

2.1. Insect Rearing. Experiments were conducted with *S. littoralis* taken from a stock that was reared in the laboratory away from any insecticidal contamination at the Department of Applied Entomology and Zoology, Faculty of Agriculture, Alexandria University, Egypt, on castor bean leaves, *Ricinus communis* L. (Malpighiales: Euphorbiaceae), under constant conditions of 25 ± 2 °C and RH 65 ± 5%.

2.2. Chemicals. Cyromazine (Trigard 75% WP) was purchased from Syngenta Agro Co., Switzerland. All solvents and reagents used in the experiments were of HPLC grade.

2.3. Nanoparticle Preparation. *2.3.1. Tungsten Oxide NPs.* 0.5 M Na_2WO_4 solution was prepared as described by Elnouby et al.[36] Briefly, sodium tungstate dehydrate ($Na_2WO_4 \cdot 2H_2O$ >98%, Sisco, India) was dissolved in deionized water. A column was packed with 30 mL ion-exchange resin (Rohm & Haas, France). This column was washed several times with water before 10 mL of the (0.5 M Na_2WO_4) solution was loaded onto the column to form a yellowish and transparent tungstic acid (H_2WO_4) solution. The obtained solution was aged at 25 ± 2 °C for 24 h to produce precipitated tungsten oxide NPs.

2.3.2. Iron Oxide NPs. Magnetic nanoparticles (MNPs) were prepared via a one-pot hydrothermal reaction described by Peng et al.[43] 4 g of iron metal powder was mixed with 10 g of NaOH in 40 mL of water for 10 min. The mixture was transferred into a Teflon-lined steel autoclave container and aged in an oven at 120 °C for 24 h. The obtained powder was washed several times with distilled water and dried overnight at 60 °C.

2.3.3. Copper-Doped Iron Oxide Nanocomposites. MNP-Cu were prepared via a one-pot hydrothermal reaction. 4 g of iron metal powder was mixed with 10 g of NaOH in 40 mL of 0.1 M copper nitrate solution for 10 min. The mixture was transferred into a Teflon-lined steel autoclave container and aged in an oven at 120 °C for 24 h. The obtained powder was washed several times with distilled water and dried overnight at 60 °C.

2.4. Characterizations of NPs. Several characterization tools were used to characterize the obtained NPs. Scanning electron microscopy (SEM, JEOL, JSM-6360LA, Japan) was used to investigate the morphological structures of the obtained materials. Transmission electron microscopy (TEM, JEOL, JEM2100 plus, Japan) was used to explore the structural properties of the prepared materials. The crystallographic phases of the produced samples were determined by powder X-ray diffraction (XRD, Shimadzu-7000, Japan). A Bruker ALPHA spectrometer (Bruker Corporation, Rheinstetten, Germany) performed Fourier transform infrared (FT-IR).

2.5. Tested Concentrations. After the toxicity tests of serial concentrations of cyromazine alone and each nanoparticle against different stages of *S. littoralis*, the combinations of cyromazine (25, 50, and 100 mg/L) and each nanomaterial (100 and 500 mg/L) were determined. Cyromazine concentrations were diluted in distilled water only, whereas WO_3 was dissolved in NaOH (0.2%) and MNPs and MNP-Cu concentrations were dissolved in HCl (0.2%).

2.6. Biological Aspects. The biological effects of cyromazine alone and its mixtures with tested NPs were assessed on *S. littoralis* using the leaf dipping assay, and three replicates were carried out (100 larvae/replicate) for each treatment. Larval duration (days), pupal duration (days), percentage pupation, and percentage adult emergence were recorded; the larval, pupal, and adult deformities were also spotted. The weight and length of fourth instar larvae were estimated for control and treatment to investigate the growth inhibition effect of the tested materials.

2.7. Biochemical Assays. *2.7.1. Sample Preparation.* The fourth instars of *S. littoralis* were exposed to various concentrations of cyromazine and its combinations with NPs. The treated and untreated larvae were homogenized with 10 volumes (w/v) of ice-cold 0.1 M sodium phosphate buffer (pH 7.5) at 96 h post-treatment. The homogenates were centrifuged at 4 °C for 30 min at 12,000 rpm using a Cryofuge 20−3 Heraeus Christ centrifuge. The enzyme activity and total protein content were determined by using the supernatants. The method of Lowry et al.[44] was used to assess the protein contents using bovine serum albumin (BSA) as a reference protein to generate the standard curve.

https://doi.org/10.1021/acsomega.3c06134
ACS Omega 2023, 8, 44867−44879

Table 1. Treatments, Nanoparticle Concentrations, and Abbreviation of Treatments Used[a]

no.	treatments	nanomaterial conc. (mg/L)	cyromazine conc. (mg/L)	abbreviation of treatments	abbreviation of poll treatments	dd-PCR	Q-PCR
1	control			**C**		+	+
2			25			−	−
3	cyromazine		50	**T1**	**P1**	+	+
4			100			−	−
5		100	25			−	−
6			50	**T2**	**P2**	+	+
7	cyromazine + WO_3		100			−	−
8			25			−	−
9		500	50	**T3**	**P3**	+	+
10			100			−	−
11			25			−	−
12		100	50	**T4**	**P4**	+	+
13	cyromazine + MNP		100			−	−
14			25			−	−
15		500	50	**T5**	**P5**	+	+
16			100			−	−
17			25			−	−
18		100	50	**T6**	**P6**	+	+
19	cyromazine + MNP-Cu		100			−	−
20			25			−	−
21		500	50	**T7**	**P7**	+	+
22			100			−	−

[a]WO_3, tungsten oxide nanoparticles; MNP, iron oxide nanoparticles; and MNP-Cu, Cu-doped iron oxide nanoparticles.

Table 2. Primer Sequences of dd-PCR and Q-PCR Used in This Study

	dd-PCR		Q-PCR	
no.	primer names	primer sequences 5̀-----3̀	gene names	primer sequences 5̀-----3̀
1	RAPD2	ATGCCCCTGT	IL-18F	ATCGCTTCCTCTCGCAACAA
			IL-18R	CTTCTACTGGTTCAGCAGCCATCT
2	RAPD3	CAGGGGACGA	IL-1α F	CGCCAATGACTCAGAGGAAGA
			IL-1α R	AGGGCGTCATTCAGGATGAA
3	RAPD4	CCTTGACGCA	IL-1βF	AATCTGTACCTGTCCTGCGTGTT
			IL-1β R	TGGGTAATTTTTGGGATCTACACTCT
4	RAPD6	AAAGCTGCGG	IL-1F8	ACCACCATCTGATCTATCTTGTTCTCT
			IL-1R8	GTGCTGCCTCCCGTTGTG
5	RAPD8	ACCTGAACGG	IL-19F	AGGAAGGGCCGTCTATCAATC
			IL-19R	GAACTGCCACAAGGTTCTGAC
6	RAPD10	GAGAGCCAAC	IL-8F	CTTGGCAGCCTTCCTGATTT
			IL-8R	TTCTTTAGCACTCCTTGGCAAAA
			β-actin F	ATGCCATTCTCCGTCTTGACTTG
			β-actin R	GAGTTGTATGTAGTCTCGTGGATT

2.7.2. GST Activity Assay. The activity of GST was determined using 1-chloro-2, 4-dinitrobenzene (CDNB), and reduced GSH as substrates, according to Kao et al.[45] with slight modifications. 0.1 mL of CDNB (25 mM), 1 mL of phosphate buffer (pH 7.5), and 1.6 mL of distilled water were added. The reaction was started by adding 0.1 mL of diluted enzyme solution (the stock solution was diluted 10-fold with 0.1 M sodium phosphate buffer, pH 7.5). Following incubation of the reaction mixture at 37 °C for 5 min, 0.1 mL of 20 mM GSH was added. The 340 nm optical density was measured for 3 min at 30-s intervals. The enzyme activity was determined using an extinction value of 9.6 mM cm^{-1} for CDNB. The specific activity was expressed as μmol of CDNB conjugate formed/min/mg protein.

2.7.3. Alpha-Esterase Activity Assay. The α-esterase activity was estimated using α-naphthyl acetate as the substrate by Van Asperen[46] and Chen et al.[47]. 0.1 mL of diluted enzyme sample (10 times with 0.1 M sodium phosphate buffer) was added to 2 mL of 1.5 mM α-naphthyl acetate solution. This mixture was incubated for 30 min at 25 °C. The addition of fast blue B (in 5% SDS) staining solution stopped the reaction. After incubation for 15 min, the absorbance at 490 nm was measured. The concentration of the hydrolyzed substrate was calculated using the α-naphthol standard curve. Specific activity was reported regarding μmol of α-naphthol produced/min/mg protein.

2.8. Differential Display Polymerase Chain Reaction (dd-PCR). *2.8.1. Total RNA Extraction.* The larva was ground to a fine powder using liquid nitrogen from seven larvae's {(treatments: control, T1, T2, T3, T4, T5, T6, and T7) and (poll treatments: P1, P2, P3, P4, P5, P6, and P7)} as shown in Table 1, and total RNA was extracted using TRIzol (Thermo

https://doi.org/10.1021/acsomega.3c06134
ACS Omega 2023, 8, 44867−44879

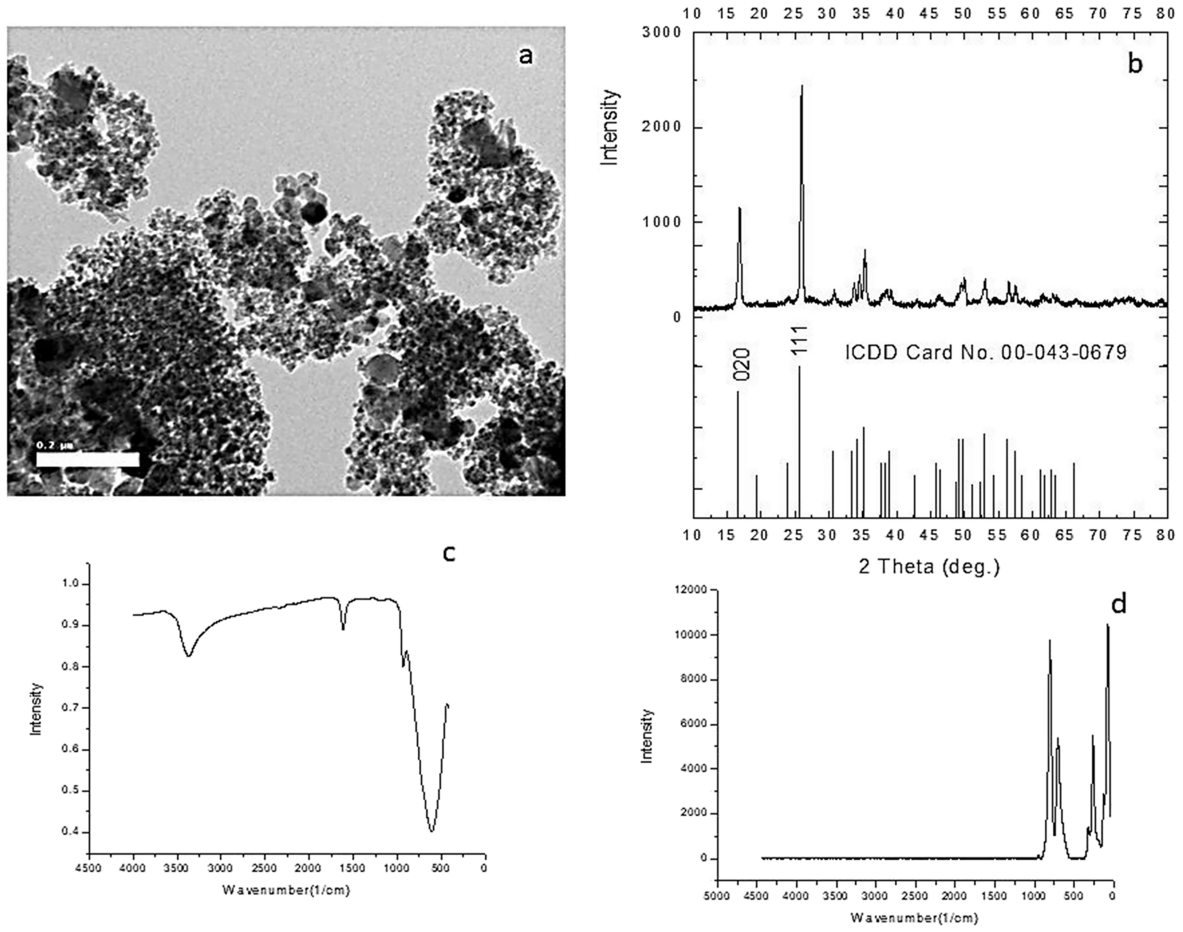

Figure 1. Structural characterizations of prepared tungsten oxide (WO_3) nanoparticles (a) TEM, (b) XRD, (c) FT-IR, and (d) Raman.

Fisher, Waltham, MA, USA) according to the manufacturer's instructions and as described in our previous study.[48,49] The obtained RNA was dissolved in diethyl dicarbonate-treated water, incubated with DNase for 1 h at 37 °C to remove any DNA residues, and quantified using a NanoDrop 1000 spectrophotometer (Thermo Scientific).

2.8.2. Reverse Transcription (cDNA Synthesis). With a total volume of 25 μL, the reaction mixture contained RNA (3 μL), 10 mM dNTPs (2.5 μL), 10× buffer with $MgCl_2$ (2.5 μL), oligo (dT) primer (4 μL), and reverse transcriptase enzyme (Biolabs) (0.2 μL). The PCR was carried out using a SureCycler 8800 thermocycler at 37 °C for 2 h and 65 °C for 20 min.

2.8.3. dd-PCR Assay. Six different primers were used to differentiate the genetic stability of the cDNA from 15 larva samples (concentration = 50 mg/L from each treatment for each group) and the pool reaction (three concentrations per treatment; 25, 50, and 100 mg/L together) was prepared for dd-PCR of each group, as shown in Table 1, which were under our study. Sequences of primers are illustrated in Table 2. In the dd-PCR reaction with a total volume of 25 μL, the reaction mixture contained 10× buffer (5 μL), 10 pmol primer (5 μL), 25 mM $MgCl_2$ (2.5 μL), 10 mM dNTPs (2 μL), cDNA (1 μL), and Taq DNA polymerase (0.2 μL) (Promega).[49] The dd-PCR was carried out using a SureCycler 8800 thermocycler (Agilent Technologies), with one cycle at 95 °C for 3 min, 40 cycles (95 °C for 45 s, 30 °C for 60 s, 72 °C for 1 min), and the final cycle at 72 °C for 5 min. The dd-PCR products were separated using 2% agarose gel electrophoresis with a DNA marker and photographed using a gel documentation system.

2.8.4. Q-PCR Assay. The effects of nanomaterials on larval interleukin genes were evaluated using q-PCR. A different set of primers (Table 2) specific to IL-18, IL-1α, IL-1β, IL-1F, IL-19, and IL-8 genes were used in this study. The housekeeping gene β-actin (Table 2) was used as a reference gene to normalize the transcript expression levels. Each group's treatments (control, T1, T2, T3, T4, T5, T6, and T7) were prepared for q-PCR analysis. Reactions of each sample were run in triplicate using Rotor-Gene 6000 (QIAGEN, ABI System, Hilden, Germany) with the SYBR Green PCR Master Mix (Fermentas, Waltham, MA, USA).[50,51] The amplification program and relative expression level of the target gene were accurately quantified and calculated, as described previously.[52]

2.9. Statistical Analysis. One-way analysis of variance (ANOVA) was used to compare the differences between the means of the treatments with the Tukey's honest significant difference (HSD) test; $P < 0.05$ was considered significant.[53]

3. RESULTS

3.1. Structural Characterizations of NPs. *3.1.1. Tungsten Oxide NPs.* In the TEM micrograph of the prepared tungsten oxide NPs, it is clear that the obtained NPs are in uniform spherical shape (Figure 1a). The XRD pattern of the prepared tungsten oxide NPs shows a single phase where all peaks are indexed to the orthorhombic $WO3{\cdot}H_2O$, with a space group of *Pmnb* (62) and lattice parameters: a = 5.2380

https://doi.org/10.1021/acsomega.3c06134
ACS Omega 2023, 8, 44867−44879

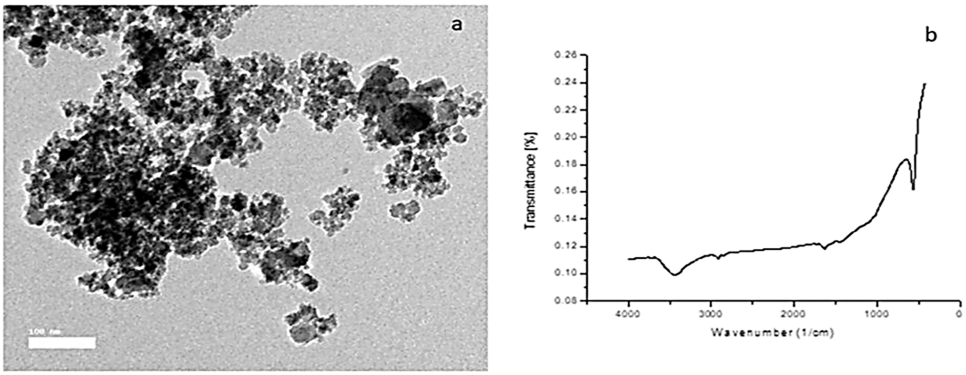

Figure 2. Structural characterizations of prepared iron oxide nanoparticles (MNP) (a) TEM and (b) FT-IR.

Å, b = 10.7040 Å, and c = 5.1200 Å (ICDD Card No. 00−043−0679) as shown in (Figure 1b). The FT-IR spectra of the prepared tungsten oxide NPs demonstrate the intense broad band at 3406 cm^{-1} reveaing the stretching motion of (O−H), and the medium narrow band at 1616 cm^{-1} is characteristic of in plane bending δ (H−O−H) of the water molecule. A very intense broad band in the region 902−621 cm^{-1} corresponds to different motions arising from W−O linkage.[54] Therefore, the band at 902 cm^{-1} refers to the stretching of (W═Ot) (where Ot is the terminal oxygen). The bands at 763 and 694 cm^{-1} revealed the stretching (W−O) and the band at 713 cm^{-1} due to stretching (W−O−W) (Figure 1c). Peaks at 75 and 128 cm^{-1} in the Raman spectra of the produced tungsten oxide NPs can be assigned to vibrational modes of block chains into the lattice of WO_3.[55] The two bands observed at 261 and 322 cm^{-1} have been assigned to O−W−O bending modes of the bridging oxide.[56] While two other bands observed at 704 and 806 cm^{-1} are the corresponding stretching modes (Figure 1d).

3.1.2. Iron Oxide NPs. In the TEM micrograph of the prepared MNP, it is clear that the obtained NPs are in a polygon shape with a size distribution from 15 to 70 nm (Figure 2a). The FT-IR spectrum of the MNP shows that the dominating signal at 567 cm^{-1} is due to Fe−O, which confirms the formation of iron oxide (Fe_3O_4).[57] While the peak at 1631 cm^{-1} is corresponding to O−H bending, which confirmed the presence of hydroxyl groups on the MNP surfaces. The peak observed at 3437 cm^{-1} is ascribed to O−H starching, indicating the presence of water molecules (Figure 2b).

3.1.3. Copper-Doped Iron Oxide NPs. In the TEM micrograph of MNP-Cu (Figure 3), it is noticeable that the obtained product is composed of large crystals with a relatively uniform, square morphology,[58] and the wide range of crystal size explained the effect of Cu ions on the growth behavior of magnetic NPs, compared to pure magnetic NPs (see Figure 2).

3.2. Biological Aspects of the Tested Materials. Effects of the insecticide cyromazine and its mixtures with tested NPs on the biological aspects of *S. littoralis* were evaluated. The larval duration, pupal duration, pupation percent, adult emergence percent, and some malformations were assessed. The results showed that the larval and pupal durations were significantly increased under all treatments compared with the control. The larval and pupal durations increased exponentially with increasing concentrations of cyromazine and nanomaterials. The longest larval and pupal periods were recorded under treatment with the mixture of cyromazine (100 mg/L) and MNP-Cu (500 mg/L); the survival periods were 23.5 and 15.6

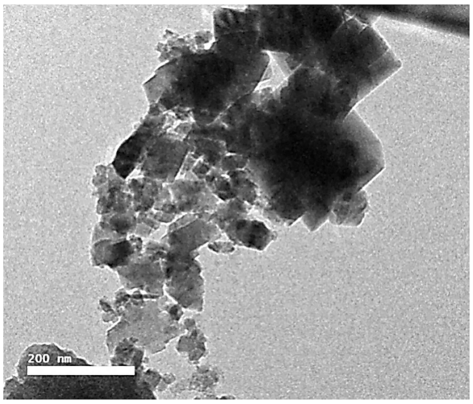

Figure 3. TEM micrograph of Cu-doped iron oxide nanoparticles (MNP-Cu).

days, respectively, followed by the mixtures of cyromazine and MNP (Figure 4). The percentage of pupation and adult emergence were negatively affected by all treatments. Regarding the pupation percent, the mixtures of cyromazine (100 mg/L) + MNP-Cu (500 mg/L) caused the highest reduction in pupation percentages, 24.6%, followed by no significant difference between the mixtures of cyromazine (100 mg/L) + MNP (500 mg/L) and cyromazine (100 mg/L) + WO_3 (500 mg/L). Adult emergence was strongly affected by all treatments. No adult emergence was recorded under treatment by mixtures of 500 mg/L nanomaterials, except the mixture of cyromazine (25 mg/L) + WO_3 (500 mg/L), which recorded 27.3% of adult emergence (Figure 5). Some malformations were reported in *S. littoralis* stages after treatment with the tested materials (Figure 6).

The body length and weight of the fourth instars of *S. littoralis* larvae after being affected by cyromazine and its mixtures with three nanomaterials were further determined in Table 3 and Figure 7. It was clear that larval length and body weight decreased progressively as the concentration of nanomaterials increased. The *S. littoralis* fourth larvae, after treatment with the MNP-Cu/cyromazine mixtures, had a significantly smaller length and lighter body weight than the control and cyromazine treatments. The most effective mixture was cyromazine (100 mg/L) + MNP-Cu (500 mg/L), with the mean larval length and body weight being 0.64 and 45.62 mg, compared with 1.86 and 145.3 mg in the control, respectively.

3.3. Detoxification Enzyme Activities of *S. littoralis*. The effect of cyromazine and its mixtures with three nanomaterials on GST and α-esterase enzyme activities are

https://doi.org/10.1021/acsomega.3c06134
ACS Omega 2023, 8, 44867−44879

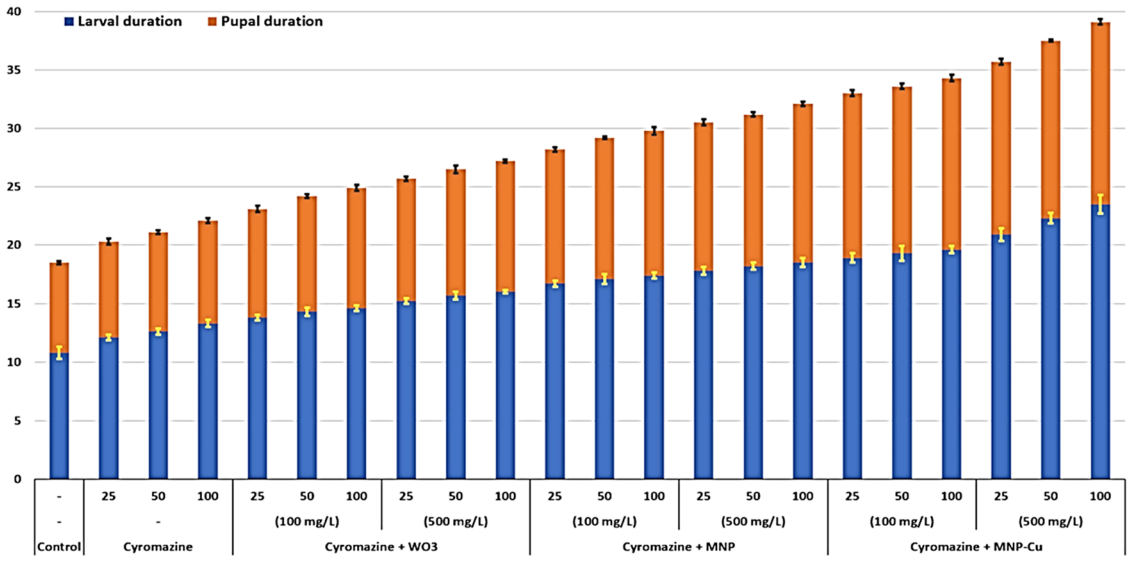

Figure 4. Effect of cyromazine and its mixtures with tungsten oxide (WO_3), iron oxide nanoparticles (MNP), and Cu-doped iron oxide nanoparticles (MNP-Cu) at 100 and 500 mg/L on larval and pupal durations of *S. littoralis*.

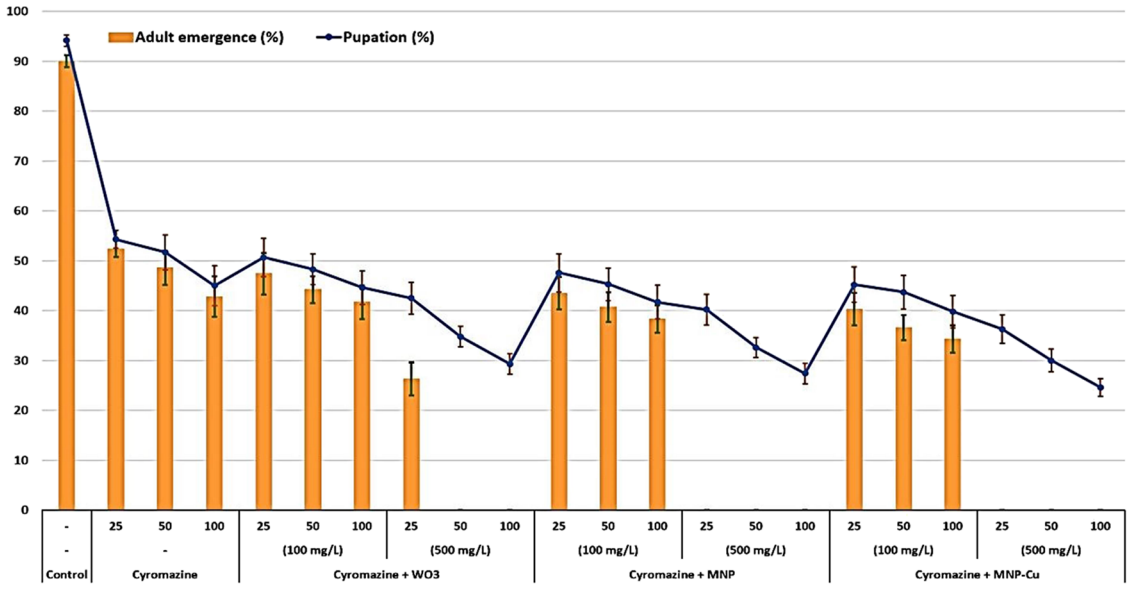

Figure 5. Effect of cyromazine and its mixtures with tungsten oxide (WO_3), iron oxide nanoparticles (MNP), and Cu-doped iron oxide nanoparticles (MNP-Cu) at 100 and 500 mg/L on pupation and adult emergence percentages of *S. littoralis*.

illustrated in Figure 8. The cyromazine treatments' GST and α-esterase enzyme activities of *S. littoralis* were significantly higher than those of the mixtures with three tested nanomaterials. Mixing cyromazine with nanomaterials decreased its excitatory effect on enzymatic activities. Cyromazine alone at 25, 50, and 100 mg/L, had the highest induction; GST activity was 203.4, 205.5, and 210.4 μmol/min/mg protein, respectively, compared with 114.4 μmol/min/mg protein in control. However, the mixture of cyromazine (100 mg/L) with MNP-Cu (500 mg/L) was 198.3 μmol/min/mg protein. The α-esterase activity of *S. littoralis* after being treated with cyromazine alone at 100 mg/L was 523.7 μg of α-naphthol/min/mg protein compared with 270.4 μg of α-naphthol/min/mg of protein in the control, followed by the mixtures of cyromazine + MNP-Cu.

3.4. Molecular Characterization. *3.4.1. dd-PCR.* Based on the up and downregulated genes in dd-PCR, the band pattern obtained by the primer rapid 2 showed that the treatment (T) samples were divided into three different groups compared to the control group. Samples T1 and 2 formed their groups, while samples T7 and 3 formed a separate group. Each of the T4 and 5 samples formed its own group. In the case of sample P, samples were separated into four groups; the first group included samples P1, 2, 3, and 5. While each of the remaining three samples, P4, 6, and 7, was separated into its own group (Figure 9A). Primer rapid 3 differentiated the examined samples, dividing T samples into three groups and P into four others. The first group included samples T1 and 2, the second group included samples T3 and 5, and the third group contained samples T6 and 7. In the case of P samples, the first group included samples P1, 3, 4, and 5, while the others, P2, 6, and 7, were separated into three different groups (Figure 9B).

https://doi.org/10.1021/acsomega.3c06134
ACS Omega 2023, 8, 44867−44879

Figure 6. Some malformations of *S. littoralis* stages are affected by cyromazine's larval applications and its nanomaterials' mixtures; control normal 4th instar larvae (A), normal pupa (D), and normal adult (G). Larva resulted from treatment with cyromazine alone (B), deformed mouthparts and unpigmented cuticle parts from the abdominal region. Larva treated with the mixture of cyromazine + MNP-Cu (C) with enlargement and curvature in the thorax, absence of the thoracic legs, and hardening of the cuticle in the first thoracic segment. Uncompleted pupation for larva treated with cyromazine alone (E), intermediate larval-pupal stage resulting from treated lava by the mixture cyromazine + MNP-Cu (F). Adults failed to emerge from the pupal stage due to the larvae treatment by cyromazine alone (H) and the mixture of cyromazine + MNP-Cu (I).

In primer rapid 4, it was able to divide the treatments into four different groups compared with the control group (Figure 9C). The first group included treatments T1, 2, 3, and 6. The other three treatments formed three separate groups. In the same context, treatments P were divided into four separate groups; the first group contained P1 and 2, while P3, 4, and 5 formed the second group, and the remaining treatments, P6 and 7, were separated into their own group (Figure 9C). While primer rapid 6 grouped the T treatments into three groups compared with the control. Samples T1, 3, and 4 were located in one group, and samples T2 and 7 were separated into another group, but sample T5 formed a unique group (Figure 9D). In the case of P samples, the samples were grouped as follows: the first group included the two samples, P1 and 3, and the second group included the samples P2 and 4, while the third and last group included the samples P5, 6, and 7, respectively (Figure 9D).

However, primer rapid 8 divided the T samples into three groups, and for the first time, the control group and T1 were collected in one group. At the same time, the T2 and 3 samples formed another group. The four treatments, T4, 5, 6, and 7, were separated into their own groups (Figure 9E). On the other hand, the P treatments were divided into four groups; the first group was P2, 4, and 7, and the second was P5 and 6. However, each P1 or 3 was separated into groups (Figure 9E). Like its counterpart, the primer rapid 10 combined the control group with the T2 and 3 treatments in one group. Samples T4, 6, and 7 formed one group (Figure 9F). T1 and T5 were each separated into their own group. In the case of P treatments, primer rapid 10 divided the examined samples into three groups; the first group included samples P2, 3, 4, and 5. The second group consisted of samples P6 and 7, while sample B1 was separated into its own group (Figure 9F).

The dd-PCR results generally revealed many up and downregulated genes in the treated insects compared to the control. Primers 2, 3, and 6 on the T2 and P6 constructs show this to be the case in insect treatments. Primers 8 and 10 found a small number of upregulated genes, which showed up only after T4 and P6 treatments. Research suggests that this impact may increase the insect's resistance to disease. This was obvious because when just nanomaterials were used, the larval mortality rate was not reported. Still, when nanomaterials were mixed with the insecticide, the percentage of dead insects increased, though that percentage remained lower than the percentage obtained from the insecticide itself. It can be said that the nanomaterials tested in this paper did not have any toxic effect on the insects; they rather increased their immune system and reduced the percentage of toxicity of the insecticide on the insect in its different stages of growth, specifically in the stages of larva and pupa.

3.4.2. QRT-PCR Analysis. Studying the gene expression of samples using interleukin 18 (Figure 10) showed that the gene expression was highest with seven treatments, followed by T5, 4, 6, and 2, respectively. The gene expression of sample T3 was relative to or equal to that of the control sample, while the gene expression was reduced to the lowest level with sample T1. The results obtained with the interleukin alpha gene showed that the gene expression of all treatments was similar to that of the control except for sample 6, where the gene expression was very weak compared to that of the control or other samples.

In the case of interleukin and beta, the gene expression of the treatments was variable and did not have a specific pattern; it was found that the gene expression of the control group was equal or close to the gene expression of treatments 2, 4, and 5, yet this expression was less with treatments 1, 3, and 7 when compared with the control or the gene expression of other treatments. On the other hand, sample 6 showed a higher gene expression than everyone else (Figure 10).

On the other hand, the interleukin 1F results showed that the gene expression of samples 6, 3, and 2 may approximate the gene expression of the control group, respectively. This gene expression has been reduced to the lowest level or may be absent with treatment No. 4. The gene expression of samples 5, 1, and 7 jumped to the highest level compared to the control group, respectively. In the case of interleukin 19, the results shown in samples 1 and 5 showed that the gene expression was close to or equal to that of the control sample. This expression was at the highest level for samples 2, 4, 3, and 7, respectively, as shown in Figure 10. Sample 6 had significantly lower gene expression compared to the control group or other samples. In the case of interleukin 8, it was shown that the gene expression of all samples was highly correlated to the control group, though the highest gene expression was found in samples 3, 2, 1, and 5, respectively (Figure 10).

https://doi.org/10.1021/acsomega.3c06134
ACS Omega 2023, 8, 44867−44879

Table 3. Effect of Cyromazine and Its Mixtures with WO_3, MNP, and MNP-Cu on the Larval Length, and Body Weight of 4th Instars of *S. littoralis*[a]

treatment	nanomaterials conc. (mg/L)	cyromazine conc. (mg/L)	larval length (cm) ± SE	larval body weight (mg) ± SE
control			1.86^{a} ± 0.012	145.03^{a} ± 1.66
cyromazine		25	0.95^{b} ± 0.018	68.60^{b} ± 1.70
		50	0.93^{bc} ± 0.015	67.43^{bc} ± 2.08
		100	0.92^{bcd} ± 0.020	66.17^{bcd} ± 1.96
cyromazine + WO_3	100	25	0.90^{bcde} ± 0.026	65.13^{bcde} ± 1.91
		50	0.89^{cdef} ± 0.023	64.40^{bcde} ± 2.12
		100	0.87^{defg} ± 0.020	63.27^{cdef} ± 1.31
	500	25	0.85^{efgh} ± 0.017	62.76^{def} ± 0.88
		50	0.84^{fgh} ± 0.018	61.10^{efg} ± 1.28
		100	0.82^{ghi} ± 0.015	59.36^{fgh} ± 1.04
cyromazine + MNP	100	25	0.81^{hij} ± 0.017	58.20^{ghi} ± 1.27
		50	0.80^{hijk} ± 0.026	56.63^{hij} ± 1.52
		100	0.78^{ijkl} ± 0.015	55.30^{hij} ± 1.70
	500	25	0.76^{jklm} ± 0.017	54.26^{ijk} ± 1.09
		50	0.75^{klm} ± 0.022	53.47^{jkl} ± 1.44
		100	$0.73l^{mn}$ ± 0.015	52.70^{jklm} ± 1.15
cyromazine + MNP-Cu	100	25	0.72^{mno} ± 0.018	50.83^{klmn} ± 0.75
		50	0.71^{mno} ± 0.023	49.36^{lmno} ± 1.85
		100	0.69^{nop} ± 0.017	48.50^{mno} ± 1.76
	500	25	0.67^{op} ± 0.021	46.97^{no} ± 1.82
		50	0.65^{p} ± 0.017	46.23^{o} ± 1.74
		100	0.64^{p} ± 0.018	45.62^{o} ± 1.40

[a]WO_3, tungsten oxide nanoparticles; MNP, iron oxide nanoparticles; and MNP-Cu, Cu-doped iron oxide nanoparticles. Means followed by different lowercase letters within the same column denote significant differences at $P < 0.05$. SE means standard error.

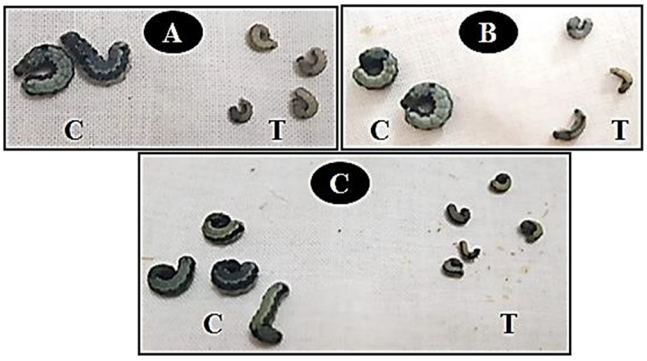

Figure 7. Effect of treatment (T) by cyromazine (A) and its mixture with iron oxide nanoparticles (MNP) (B) and with Cu-doped iron oxide nanoparticles (MNP-Cu) (C) on the larval length and body weight of 4th instar larvae of *S. littoralis* compared with control (C).

4. DISCUSSION

Nanopesticides have positively impacted the control of plant pests and diseases by delivering the active ingredient to the plant in a controlled way. This smart delivery provides sustainable solutions and reduces the amount and cost of fertilizers and pesticides for farmers.[59] In the present study, the tested nanomaterials alone have no toxicity against *S. littoralis* stages; these findings much agree with the findings which found that no significant genotoxicity or cytotoxicity existed in MNP-treated water, where MNPs have great potential in experimental drinking water treatment to remove pathogenic bacteria.[60] On the other hand, some studies disagree with the present results, which clarified that exposure to a highly concentrated dose of Ch-Fe_3O_4 NPs leads to high larval mortality.[61] Previous research works have reported acute intoxication of *Drosophila melanogaster* with iron ($FeSO_4$) and proved to diminish fly survival and locomotor activity, including climbing capabilities.[62]

The use of tested nanomaterials as an additive compound to the insecticide aims to reduce the insecticide dosage and thus reduce the impact on the environment by increasing its effectiveness, not by increasing the insecticide toxicity but by interfering with the other aspects of the pest, such as the biological, behavioral, and physiological aspects. The antagonistic effect of the tested nanomaterials was confirmed, and they grew with increasing concentrations. The tested magnetic nanomaterials decreased the insecticidal effect of cyromazine; this result agreed with Saeidi et al.,[63] which approved the unique adsorption properties of the magnetic nanomaterials due to different distributions of reactive surface sites and disordered surface regions that may explain the antagonistic effect of the tested nanomaterials. The dose concentration of Ch-Fe_3O_4 NPs showed a shortening of lifespan and decreased larval survival associated with the toxic effect against larvae and adults of *D. melanogaster*.[61] Abraham et al.[27] studied the effects of Fe_3O_4 NPs during the development of the tephritid flies *Ceratitis capitata* and *Anastrepha fraterculus*. They found that only 40% of larvae feeder medium at 400 μg/mL Fe_3O_4 NPs could continue their life cycle, in contrast to 92% of the control.

We found larvae having difficulties in advancing to the next stage of development; this was agreed with Chen et al.[64] who found that *Drosophila* uptake of NPs caused a significant decrease in the development and *Drosophila* female flies exhibited an adverse response and developmental delay at the egg-pupae and pupae-adult transitions. Also, silver NPs significantly decreased the likelihood of lifespan (eggs to pupate) and reduced the percentage of adult emergences.[65]

The present results revealed a delay in growth, a decrease in larval size, and some malformations caused by the MNP

https://doi.org/10.1021/acsomega.3c06134
ACS Omega 2023, 8, 44867−44879

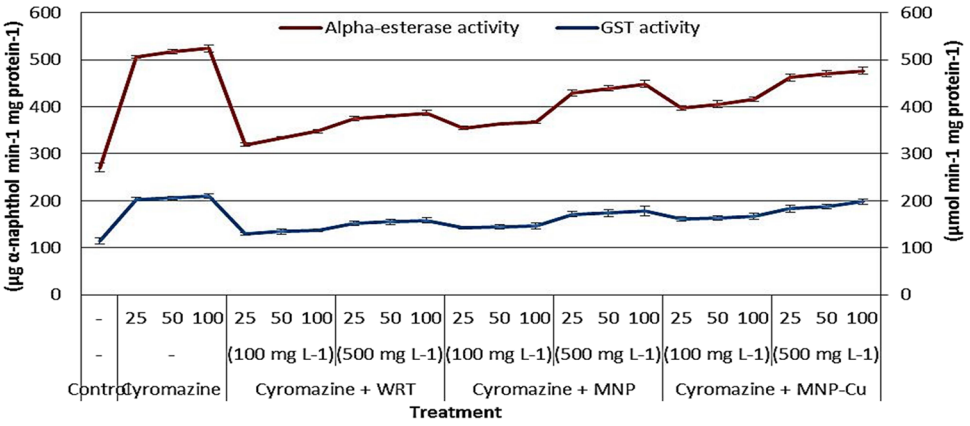

Figure 8. Effect of cyromazine and its mixtures with tungsten oxide (WO_3), iron oxide nanoparticles (MNP), and Cu-doped iron oxide nanoparticles (MNP-Cu) on glutathione *S*-transferase (GST) and α-esterase activities of *S. littoralis* 4th instar larvae.

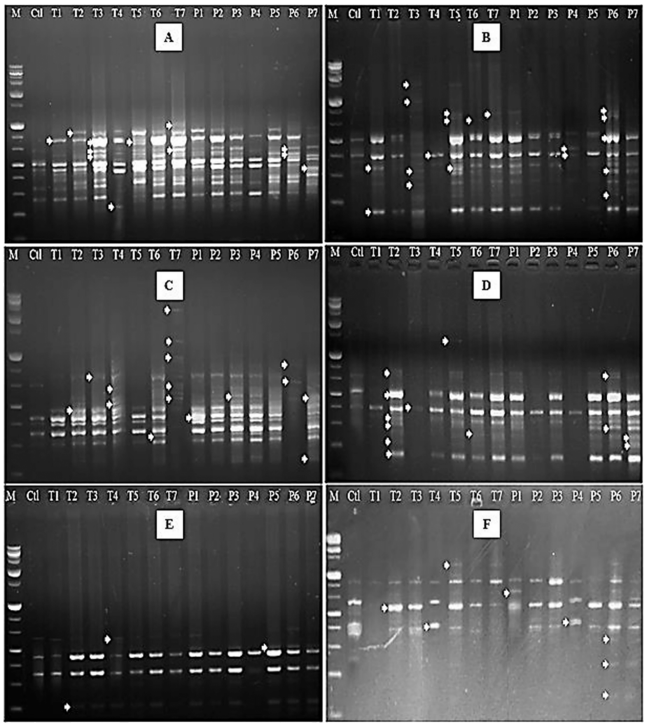

Figure 9. Gene expression of dd-PCR using different arbitrary primers; (A) RAPD 2; (B) RAPD 3; (C) RAPD 4; (D) RAPD 6; (E) RAPD 8; and (F), RAPD 10, respectively. M, 1.5 Kbp DNA marker; Ctl, untreated larva; T1, cyromazine (50 mg/L); T2, cyromazine (50 mg/L) + WO_3 (100 mg/L); T3, cyromazine (50 mg/L) + WO_3 (500 mg/L); T4, cyromazine (50 mg/L) + MNP (100 mg/L); T5, cyromazine (50 mg/L) + MNP (500 mg/L); T6, cyromazine (50 mg/L) + MNP-Cu (100 mg/L); T7, cyromazine (50 mg/L) + MNP-Cu (500 mg/L); then, poll treatments P1, cyromazine (25, 50, and 100 mg/L); P2, cyromazine (25, 50, and 100 mg/L) + WO_3 (100 mg/L); P3, cyromazine (25, 50, and 100 mg/L) + WO_3 (500 mg/L); P4, cyromazine (25, 50, and 100 mg/L) + MNP (100 mg/L); P5, cyromazine (25, 50, and 100 mg/L) + MNP (500 mg/L); P6, cyromazine (25, 50, and 100 mg L) + MNP-Cu (100 mg/L); and P7, cyromazine (25, 50, and 100 mg/L) + MNP-Cu (500 mg/L).

treatment; this corresponds with the results, which showed that short-term exposure to a concentration of Fe_3O_4 NPs at 100 μg/mL is sufficient to cause lasting and harmful effects on the life cycle traits of *C. capitata* and *A. fraterculus*.[66−70] Also, they reported delays in growth, abnormalities of wings, and the alteration and interruption of the life cycle. *D. melanogaster* newborn flies presented toxicity symptoms such as imperceptible movement and abnormal wing and bristle phenotypes after treatment with zinc oxide.[67,69]

Magnetite NPs were produced and tested to control populations of tephritid fruit flies. The results showed that the magnetite NPs disrupt the life cycle of *C. capitata* and *A. fraterculus* by distressing their behavior and developing them, altering the phenotype of larvae and pupae, and turning off the ecdysis of pharate adult.[27]

Kang et al.[71] used dd-PCR to study the *Trichoplusiani* gene expression of the insect immune system in larval and pupa instars infected with *Enterobacter cloacae*. They concluded that dd-PCR has a high potential to demonstrate the down and upregulated genes associated with the immune state of the whole compared with the gene involved in larval development. The same observation was reported by Seufi et al.;[72] they postulated that the challenged larvae of *S. littoralis* showed upregulation of different genes in different molecular sizes, most of them being antimicrobial peptides (AMPs). In this study, about 71 upregulated genes with different molecular weights were observed, and more than 7 genes were downregulated. In another study, the *Tribolium castaneum*was treated with nanocarbon tubes coated with poly amido amine dendrimer generation 5 (PAMAM G = 5, cat. no. 536709) and showed shutdown of specific genes but without any effect on the toxicity indicator gene. Nowicki et al.[73] used Nebcolloostatin for eco-friendly pest control. They found that this type of hormone can cause immune disturbance for the treated insects and could help in insect control, especially on Tenebriomolitor. Shahzad and Manzoor[74] postulated that nanomaterials, can affect the treated insect's cuticle pigmentation and integrity, induce insect immune responses, and alter gene expression. The gene alteration resulted in altered protein, lipid, and carbohydrate metabolism, along with cellular toxicity that impairs the development and reproduction of the insect.

In this study, we found that the used nanomaterials affected gene expression and insect immune response. However, the toxicity of the used materials was weak compared to that of the other chemical insecticides. Moreover, when the examined nanomaterials were mixed with the chemical insecticides, insect deformation was observed, and the mortality percentage was not as high as expected. The nanomaterials used in this study render the toxicity of the chemical pesticides and

https://doi.org/10.1021/acsomega.3c06134
ACS Omega 2023, 8, 44867−44879

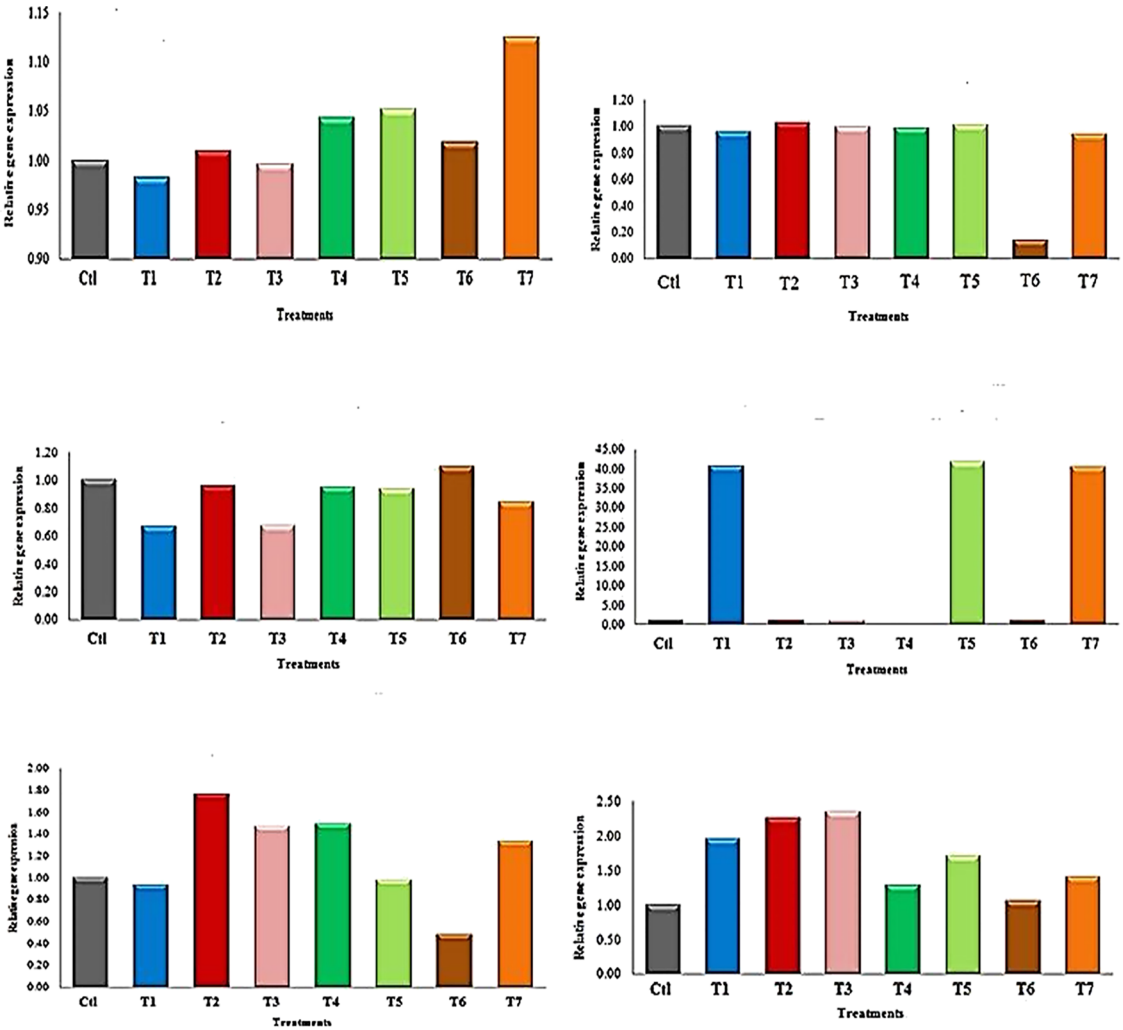

Figure 10. Relative gene expression levels of larva to interleukin genes (IL-18, IL-1α, IL-1β, IL-1, IL-19, and IL-8, respectively) for Ctl, untreated larva; T1, cyromazine (50 mg/L); T2, cyromazine (50 mg/L) + WO_3 (100 mg/L); T3, cyromazine (50 mg/L) + WO_3 (500 mg/L); T4, cyromazine (50 mg/L) + MNP (100 mg/L); T5, cyromazine (50 mg/L) + MNP (500 mg/L); T6, cyromazine (50 mg/L) + MNP-Cu (100 mg/L); and T7, cyromazine (50 mg/L) + MNP-Cu (500 mg/L).

generate individuals suffering malformation. Regarding the results obtained by the real-time PCR, the insect's immune response to the treatments starting from T1 to T7 indicate high immune response in all the treated insects compared with the control except for IL-1α. The expression was steady in all examined samples, which means that our treatments have no apoptotic effects on the treated insects.[75] The high expression of IL-18 in treated insects means that these insects can produce a high amount of interferon-γ from T-cells and natural killer cells, which means that all the examined treatments in this study make the insect immune system strong, not weak.[76] The same observation was with interleukin 1B. Still, in the case of IL-1F, the high expression with the treatments T1, 5, and 7 revealed that these three concentrations cause inflammation in the insects without killing them.[77] The high expression of IL-19 with the treatments T2, 3, 4, and 7 means that these concentrations induce the anti-inflammatory regulating genes that recently formed. Still, the T6 suppressed the anti-inflammatory effect, meaning this treatment is more effective than the others.[78] In the case of IL-8, it was observed that the gene expression profile confirms the results obtained by IL-19.

5. CONCLUSIONS

The study found that none of the tested NPs exhibited toxicity toward *S. littoralis* stages. The larval and pupal durations increased exponentially with increasing concentrations of cyromazine and nanomaterials. The percentage of pupation and adult emergence were negatively affected by all treatments. The *S. littoralis* larvae had smaller lengths and lighter body weights after treatment with MNP-Cu/cyromazine mixtures. Cyromazine treatments significantly increased *S. littoralis* GST and α-esterase enzyme activities. The insect immune response against the nanomaterials decreased the insecticides' effect. Comprehensive studies about the performance of NPs in field conditions and their toxicity to nontarget organisms should be undertaken to help develop control strategies in agricultural areas and minimize the environmental hazards.

Acknowledgment. The authors are grateful to Ms. Marwa Samy (Plant Protection and Biomolecular Diagnosis Department, Arid Lands Cultivation Research Institute) for her help in the molecular investigation.

https://doi.org/10.1021/acsomega.3c06134
ACS Omega 2023, 8, 44867−44879

■ ASSOCIATED CONTENT

Data Availability Statement

The data sets used and/or analyzed during the current study are available from the corresponding author on reasonable request.

■ AUTHOR INFORMATION

Corresponding Author

Sahar E. Eldesouky − *Cotton Pesticides Evaluation Department, Plant Protection Research Institute, Agricultural Research Center, Alexandria 21616, Egypt;* orcid.org/0000-0003-4823-9013; Email: elsayedsahar@gmail.com

Authors

Dalia G. Aseel − *Plant Protection and Biomolecular Diagnosis Department, Arid Lands Cultivation Research Institute (ALCRI), City of Scientific Research and Technological Applications (SRTA-City), New Borg El-Arab City, Alexandria 21934, Egypt*

Mohamed S. Elnouby − *Composite and Nanostructured Materials Research Department, Advanced Technology and New Materials Research Institute (ATNMRI), City of Scientific Research and Technological Applications (SRTA-City), New Borg El-Arab City, Alexandria 21934, Egypt;* orcid.org/0000-0001-9099-7198

Fatma H. Galal − *Biology Department, College of Science, Jouf University, Sakaka 72341, Saudi Arabia*

Ammar AL-Farga − *Biochemistry Department, Faculty of Science, Jeddah University, Jeddah 21577, Saudi Arabia*

Elsayed E. Hafez − *Plant Protection and Biomolecular Diagnosis Department, Arid Lands Cultivation Research Institute (ALCRI), City of Scientific Research and Technological Applications (SRTA-City), New Borg El-Arab City, Alexandria 21934, Egypt*

Hanaa S. Hussein − *Applied Entomology and Zoology Department, Faculty of Agriculture, Alexandria University, Alexandria 21545, Egypt*

Complete contact information is available at: https://pubs.acs.org/10.1021/acsomega.3c06134

Author Contributions

S.E.E., D.G.A, M.E., F.H.G., A.A.-F, and H.S.H. idea and the design of the experiments; S.E.E. and H.S.H. biological parameters, biochemical assay, data curation, formal analysis, and writing-editing and revision of the manuscript; D.G.A. molecular investigation data analysis, writing-editing, and revision of the manuscript; M.E. nanomaterials preparation and characterization; F.H.G., A.A.-F., and E.E.H. involved in conceptualization and investigation. All authors have read and agreed to the published version of the manuscript.

Notes

The authors declare no competing financial interest.

■ REFERENCES

(1) Arumugam, E.; Muthusamy, B.; Dhamodaran, K.; Thangarasu, M.; Kaliyamoorthy, K.; Kuppusamy, E. Pesticidal Activity of *Rivina humilis* L. (Phytolaccaceae) Against Important Agricultural Polyphagous Field Pest, *Spodoptera litura* (Fab.) (Lepidoptera: Noctuidae). *J. Coast. Life. Med.* **2015**, *3*, 389−394.

(2) Kumar, A.; Negi, N.; Haider, S. Z.; Negi, D. S. Composition and Efficacy of *Zanthoylum alatum* Essential Oils and Extracts Against *Spodoptera litura*. *Chem. Nat. Comp.* **2014**, *50*, 920−923.

(3) Sharma, A.; Kumar, V.; Shahzad, B.; Tanveer, M.; Sidhu, G. P. S.; Handa, N.; et al. Worldwide Pesticide Usage and Its Impacts on Ecosystem. *SN Appl. Sci.* **2019**, *1*, 1446.

(4) Woodrow, J. E.; Gibson, K. A.; Seiber, J. N. Pesticides and Related Toxicants in the Atmosphere. *Rev. Environ. Contam. Toxicol.* **2018**, *247*, 147−196.

(5) Ippolito, A.; Fait, G. Pesticides in Surface Waters: From Edge-of-Field to Global Modelling. *Curr. Opin. Environ. Sustain.* **2019**, *36*, 7884.

(6) Aydin, H.; Gürkan, M. O. The Efficacy of Spinosad on Different Strains of *Spodoptera littoralis* (Boisduval) (Lepidoptera: Noctuidae). *Turk. J. Biol.* **2006**, *30*, 5−9.

(7) Mahmood, I.; Imadi, S. R.; Shazadi, K.; Gul, A.; Hakeem, K. R. Effects of Pesticides on Environment. In: Hakeem, K.; Akhtar, M.; Abdullah, S. (eds) *Plant, Soil and Microbes*; Springer: Cham, 2016, 253−69.

(8) Srivastava, A. K.; Kesavachandran, C. *Health Effects of Pesticides*; CRC Press, 2019.

(9) Bayda, S.; Adeel, M.; Tuccinardi, T.; Cordani, M.; Rizzolio, F. The History of Nanoscience and Nanotechnology: From Chemical−Physical Applications to Nanomedicine. *Molecules* **2020**, *25*, 112.

(10) Rai, M.; Ingle, A. Role of Nanotechnology in Agriculture with Special Reference to Management of Insect Pests. *Appl. Microbiol. Biotechnol.* **2012**, *94*, 28793.

(11) Benelli, G.; Pavela, R.; Maggi, F.; Petrelli, R.; Nicoletti, M. Commentary: Making Green Pesticides Greener? The Potential of Plant Products For Nanosynthesis and Pest Control. *J. Clust. Sci.* **2017**, *28*, 3−10.

(12) Athanassiou, C. G.; Kavallieratos, N. G.; Benelli, G.; Losic, D.; Usha Rani, P.; Desneux, N. Nanoparticles For Pest Control: Current Status and Future Perspectives. *J. Pest. Sci.* **2018**, *91*, 1−15.

(13) Landa, P. Positive Effects of Metallic Nanoparticles on Plants: Overview of Involved Mechanisms. *Plant Physiol. Biochem.* **2021**, *161*, 12−24.

(14) Keratum, A. Y.; Abo, A. R. B.; Ismail, A. A.; George, M. N. Impact of Nanoparticle Zinc Oxide and Aluminum Oxide Against Rice Weevil *Sitophilus oryzae* (Coleoptera: Curculionidae) Under Laboratory Conditions. *Egy. J. Plant Pro. Res.* **2015**, *3*, 30−38.

(15) Salem, A. A.; Hamzah, A. M.; El-Taweelah, N. M. Aluminum and Zinc Oxides Nanoparticles as a New Method For Controlling The Red Flour Beetles, *Tribolium castaneum* (Herbest) Compared to Malathion Insecticide. *J. Plant Prot. Pathol.* **2015**, *6*, 129−137.

(16) Khot, L. R.; Sankaran, S.; Maja, J. M.; Ehsani, R.; Schuster, E. W. Applications of Nanomaterials in Agricultural Production and Crop Protection: A Review. *Crop Prot.* **2012**, *35*, 64−70.

(17) Wang, T.; Ai, S.; Zhou, Y.; Luo, Z.; Dai, C.; Yang, Y.; Zhang, J.; et al. Adsorption of Agricultural Wastewater Contaminated with Antibiotics, Pesticides and Toxic Metals by Functionalized Magnetic Nanoparticles. *J. Environ. Chem. Eng.* **2018**, *6*, 6468−6478.

(18) Almomani, F.; Bhosale, R.; Khraisheh, M.; Kumar, A.; Almomani, T. Heavy Metal Ions Removal from Industrial Wastewater Using Magnetic Nanoparticles (MNP). *Appl. Surf. Sci.* **2020**, *506*, No. 144924.

(19) Baragaño, D.; Alonso, J.; Gallego, J. R.; Lobo, M. C.; Gil-Díaz, M. Magnetite Nanoparticles For the Remediation of Soils Co-contaminated with As and PAHs. *Chem. Eng. J.* **2020**, *399*, No. 125809.

(20) Dhaliwal, S. S.; Singh, J.; Taneja, P. K.; Mandal, A. Remediation Techniques For Removal of Heavy Metals From The Soil Contaminated Through Different Sources: A Review. *Environ. Sci. Pollut. Res.* **2020**, *27*, 1319−1333.

(21) Ditta, A.; Mehmood, S.; Imtiaz, M.; Rizwan, M. S.; Islam, I.Soil Fertility and Nutrient Management with the Help of Nanotechnology. In Husen, A.; Jawaid, M. (Eds.), *Nanomater. Agric. For. Appl.*; 2020, 273−287.

(22) Griesche, C.; Baeumner, A. J. Biosensors to Support Sustainable Agriculture and Food Safety. *TrAC Trends Anal. Chem.* **2020**, *128*, No. 115906.

(23) Lu, Y.; Yang, Q.; Wu, J. Recent Advances in Biosensor-Integrated Enrichment Methods For Preconcentrating and Detecting the Low-Abundant Analytes in Agriculture and Food Samples. *TrAC Trends Anal. Chem.* **2020**, *128*, No. 115914.
(24) Dutta, P.. Seed Priming: New Vistas and Contemporary Perspectives. In *Advances in Seed Priming*; Rakshit, A.; Singh, H. B. Eds.; Springer: Singapore, 2018; 3−22.
(25) Arosio, P. Applications and Properties of Magnetic Nanoparticles. *Nanomaterials* **2021**, *11*, 1297.
(26) Spanos, A.; Athanasiou, K.; Ioannou, A.; Fotopoulos, V.; Krasia-Christoforou, T. Functionalized Magnetic Nanomaterials in Agricultural Applications. *Nanomaterials (Basel)* **2021**, *11*, 3106 DOI: 10.3390/nano11113106.
(27) Abraham, A. L. B.; de Ávila, M. R.; Torres, R.; Diz, V. Magnetite Nanoparticles as a Promising Non-Contaminant Method to Control Populations of Fruit Flies (Diptera: Tephritidae). *J. Appl. Biotechnol. Bioeng.* **2021**, *8*, 112−117.
(28) Wu, W.; Wu, Z.; Yu, T.; Jiang, C.; Kim, W. S. Recent Progress on Magnetic Iron Oxide Nanoparticles: Synthesis, Surface Functional Strategies and Biomedical Applications. *Sci. Technol. Adv. Mater.* **2015**, *16*, No. 023501.
(29) Senbill, H.; Hassan, S. M.; Eldesouky, S. E. Acaricidal and Biological Activities of Titanium Dioxide and Zinc Oxide Nanoparticles on The Two-Spotted Spider Mite, *Tetranychus urticae* Koch (Acari: Tetranychidae) and Their Side Effects on The Predatory Mite, *Neoseiulus californicus* (Acari: Phytoseiidae). *J. Asia Pac. Entomol.* **2023**, *26*, No. 102027.
(30) Elessawy, N. A.; Gouda, M. H.; Elnouby, M. S.; Zahran, H. F.; Hashim, A.; Abd El-Latif, M. M.; Santos, D. M. F. Novel Sodium Alginate/ Polyvinylpyrrolidone/ TiO_2 Nanocomposite for Efficient Removal of Cationic Dye From Aqueous Solution. *Appl. Sci.* **2021**, *11*, 9186.
(31) Baz, M. M.; El-Barkey, N. M.; Kamel, A. S.; El-Khawaga, A. H.; Nassar, M. Y. Efficacy of Porous Silica Nanostructure as An Insecticide Against Filarial Vector *Culex pipiens* (Diptera: Culicidae). *Int. J. Trop. Insect Sci.* **2022**, *42*, 2113−2125.
(32) Hussein, H. S.; Tawfeek, M. E.; Eldesouky, S. E. Toxicity and Biochemical Effects of Spirotetramat and Its Binary Mixtures with Nanosilica against *Aphis gossypii* Glover, *Bemisia tabaci* Gennadius and The Earthworm *Eisenia fetida*. *Alex. Sci. Exch. J.* **2022**, *43*, 107−119.
(33) Elnouby, M. S.; Taha, T. H.; Abu-Saied, M. A.; Saad, A. A.; Yasser, S. M. M.; Mohamed, H. Green and Chemically Synthesized Magnetic Iron Oxide Nanoparticles-Based Chitosan Composites: Preparation, Characterization, and Future Perspectives. *J. Mater. Sci. Mater. Electron.* **2021**, *32*, 10587−10599.
(34) Nassar, M. Y.; Ahmed, I. S.; Hendy, H. S. A Facile One-pot Hydrothermal Synthesis of Hematite (α-Fe_2O_3) Nanostructures and Cephalexin Antibiotic Sorptive Removal From Polluted Aqueous Media. *J. Mol. Liq.* **2018**, *271*, 844−856.
(35) El-Berry, M. F.; Sadeek, S. A.; Abdalla, A. M.; Nassar, M. Y. Facile, Controllable, Chemical Reduction Synthesis of Copper Nanostructures Utilizing Different Capping Agents. *Inorg. Nano-Met.* **2021**, *51*, 1418−1430.
(36) Elnouby, M. S.; Kuruma, K.; Nakamura, E.; Abe, H.; Suzuki, Y.; Naito, M. Facile Synthesis of WO3•H2O Square Nanoplates Via a Mild Aging of Ion-Exchanged Precursor. *J. Ceram. Soc. Jpn.* **2013**, *121*, 907−911.
(37) Elsayed, E. M.; Elnouby, M. S.; Gouda, M. H.; Elessawy, N. A.; Santos, D. M. F. Effect of The Morphology of Tungsten Oxide Embedded in Sodium Alginate/Polyvinylpyrrolidone Composite Beads on The Photocatalytic Degradation of Methylene Blue Dye Solution. *Materials (Basel)* **2020**, *13* (8), 1905.
(38) Moustafa, M.; Alamri, S.; Elnouby, M.; Taha, T.; Abu-Saied, M. A.; Shati1, A.; Al Kahtani, M.; Alrumman, S. Hydrothermal Preparation of TiO2-Ag Nanoparticles and its Antimicrobial Performance against Human Pathogenic Microbial Cells in Water. *Biocell* **2018**, *42* (93), 97.
(39) Pener, M. P.; Dhadialla, T. S. An Overview of Insect Growth Disruptors; Applied Aspects. Eds Dhadialla, T. S. *Adv. In Insect Phys.*; Elsevier: Oxford, 2012, *43*, 1−162.
(40) Reynolds, S. E.; Blakey, J. K. Cyromazine Causes Decreased Cuticle Extensibility in Larvae of The Tobacco Hornworm Manduca sexta. *Pestic. Biochem. Physiol.* **1989**, *35*, 251−258.
(41) Tanani, M.; Hamadah, Kh.; Ghoneim, K.; Basiouny, A.; Waheeb, H. Toxicity and Bioefficacy of Cyromazine on Growth and Development of The Cotton Leafworm *Spodoptera littoralis* (Lepidoptera: Noctuidae). *Int. J. Res. Stud. Zool.* **2015**, *1*, 1−15.
(42) Li, X.-Z.; Liu, Y.-H. Diet Influences the Detoxification Enzyme Activity of *Bactrocera tau* (Walker) (Diptera: Tephritidae). *Acta Entomol. Sin.* **2007**, *50*, 989−995, DOI: 10.16380/J.KCXB.2007.10.009.
(43) Peng, D.; Beysen, S.; Li, Q.; Jian, J.; Sun, Y.; Jiwuer, J. Hydrothermal Growth of Octahedral Fe_3O_4 Crystals. *Particuology* **2009**, *7*, 35−38.
(44) Lowry, O. H.; Rosebrough, N. J.; Farrand, A. L.; Randall, R. J. Protein Measurement with the Folin Phenol Reagent. *J. Biol. Chem.* **1951**, *193*, 265−275.
(45) Kao, C. H.; Hung, C. F.; Sun, C. N. Parathion and Methyl Parathion Resistance in Diamondback Moth (Lepidoptera: Plutellidae) Larvae. *J. Econ. Entomol.* **1989**, *82*, 1299−1304.
(46) Van Asperen, K. A. Study of Housefly Esterases by Means of Sensitive Colorimetric Method. *J. Insect Physiol.* **1962**, *8*, 401−414.
(47) Chen, R.; Guo, L.; Dang, H. Gene Cloning, Expression and Characterization of a Cold-Adapted Lipase from Psychrophilic Deep-Sea Bacterium *Psychrobacter* sp. C18. *World J. Microbiol. Biotechnol.* **2011**, *27*, 431−441.
(48) Aseel, D. G.; Mostafa, Y.; Riad, S. A.; Hafez, E. E. Improvement of Nitrogen Use Efficiency in Maize Using Molecular and Physiological Approaches. *Symbiosis* **2019**a, *78*, 263−274, .
(49) Rashad, Y. M.; Aseel, D. G.; Hafez, E. E. Antifungal Potential and Defense Gene Induction in Maize against *Rhizoctonia* Root Rot by Seed Extract of *Ammivisnaga* (L.) Lam. *Phytopathol. Mediterr.* **2018**, *57*, 73−88.
(50) Aseel, D. G.; Rashad, Y. M.; Hammad, S. M. *Arbuscular mycorrhizal* Fungi Trigger Transcriptional Expression of Flavonoid and Chlorogenic Acid Biosynthetic Pathways Genes in Tomato Against Tomato Mosaic Virus. *Sci. Rep.* **2019**b, *9*, 1−10, .
(51) Rashad, Y.; Aseel, D.; Hammad, S.; Elkelish, A. *Rhizophagus irregularis* and *Rhizoctonia solani* Differentially Elicit Systemic Transcriptional Expression of Polyphenol Biosynthetic Pathways Genes in Sunflower. *Biomolecules* **2020**, *10*, 379 DOI: 10.3390/biom10030379.
(52) Schmittgen, T. D.; Livak, K. J. Analyzing Real-Time PCR Data by the Comparative CT Method. *Nat. Protoc.* **2008**, *3*, 1101−1108.
(53) *SAS (Statistical analysis System) SAS users guide statistics*; SAS institute: Cary, North Carolina, U.S.A, 1997.
(54) Manna, C. M.; Nassar, M. Y.; Tofan, D.; Chakarawet, K.; Cummins, C. C. Facile Synthesis of Mononuclear Early Transition-Metal Complexes of K^3 Cyclo-Tetrametaphosphate ($[P_4O_{12}]^{4-}$) and Cyclo-Trimetaphosphate ($[P_3O_9]^{3-}$). *Dalton Trans.* **2014**, *43*, 1509−1518.
(55) Escalante, G.; López, R.; Demesa, F. N.; Villa-Sánchez, G.; Castrejón-Sánchez, V. H.; Vivaldo de la Cruz, I. Correlation Between Raman Spectra and Color of Tungsten Trioxide (WO_3) Thermally Evaporated from a Tungsten Filament. *AIP Adv.* **2021**, *11*, No. 055103.
(56) Senthilkumar, R.; Ravi, G.; Sekar, C.; Arivanandhan, M.; Navaneethan, M.; Hayakawa, Y. Determination of Gas Sensing Properties of Thermally Evaporated WO_3 Nanostructures. *J. Mater. Sci: Mater. Electron.* **2015**, *26*, 1389−1394.
(57) Refat, N. M.; Nassar, M. Y.; Sadeek, S. A. A Controllable One-Pot Hydrothermal Synthesis of Spherical Cobalt Ferrite Nanoparticles: Synthesis, Characterization, and Optical Properties. *RSC Adv.* **2022**, *12*, 25081−25095.
(58) Nassar, M. Y.; Aly, H. M.; Moustafa, M. E.; Abdelrahman, E. A. Synthesis, Characterization and Biological Activity of New 3-

https://doi.org/10.1021/acsomega.3c06134
ACS Omega 2023, 8, 44867−44879

substitued-4-amino-5-hydrazino-1,2,4-triazole Schiff Bases and Their Cu(II) Complexes: A New Approach to CuO Nanoparticles for Photocatalytic Degradation of Methylene Blue Dye. *J. Inorg. Organomet. Polym.* **2017**, *27*, 1220−1233.
(59) Chhipa, H.; Chowdhary, K.; Kaushik, N. Artificial Production of Agarwood Oil in *Aquilaria*sp by Fungi: A Review. *Phytochem. Rev.* **2017**, *16*, 835−860.
(60) Xu, Y.; Chengcai Li, C.; Zhu, X.; Huang, W. E.; Zhang, D. Application of Magnetic Nanoparticles in Drinking Water Purification. *Environ. Eng. Manag. J.* **2014**, *13*, 2023−2029.
(61) Vela, D.; Rondal, J.; Cárdenas, S.; Gutiérrez-Coronado, J.; Jara, E.; Debut, A.; Pilaquinga, F. Assessment of the Toxic Effects of Chitosan-Coated Magnetite Nanoparticles on *Drosophila melanogaster*. *Am. J. Appl. Sci.* **2020**, *17*, 204−213.
(62) Jimenez Del Rio, M.; Guzman Martinez, C.; Velez Pardo, C. The Effects of Polyphenols on Survival and Locomotor Activity in *Drosophila melanogaster* Exposed to Iron and Paraquat. *Neurochem. Res.* **2010**, *35*, 227−238.
(63) Saeidi, M.; Naeimi, A.; Komeili, A. Magnetite Nanoparticles Coated with Methoxy Polyethylene Glycol as an Efficient Adsorbent of Diazinon Pesticide from Water. *Adv. Environ. Technol.* **2016**, *1*, 25−31.
(64) Chen, H.; Wang, B.; Feng, W.; Du, W.; Ouyang, H.; Chai, Z.; Bi, X. Oral Magnetite Nanoparticles Disturb the Development of *Drosophila melanogaster* from Oogenesis to Adult Emergence. *Nanotoxicology* **2015**, *9*, 302−312.
(65) Gorth, D. J.; Rand, D. M.; Webster, T. J. Silver Nanoparticle Toxicity in *Drosophila*: Size Does Matter. *Int. J. Nanomedicine* **2011**, *6*, 343−350.
(66) Ovrusky, S. M.; Schliserman, P. Biological Control of Tephritid Fruit Flies in Argentina: Historical Review, Current Status, and Future Trends for Developing A Parasitoid Mass−Release Program. *Insects* **2012**, *3*, 870−888.
(67) Anand, A. S.; Prasad, D. N.; Singh, S. B.; Kohli, E. Chronic Exposure of Zinc Oxide Nanoparticles Causes Deviant Phenotype in *Drosophila melanogaster*. *J. Hazard. Mater.* **2017**, *327*, 180−186.
(68) Barik, B. K.; Mishra, M. Nanoparticles as A Potential Teratogen: A Lesson Learnt from Fruit Fly. *Nanotoxicology* **2019**, *13*, 258−284.
(69) Dan, P.; Sundararajan, V.; Ganeshkumar, H.; Gnanabarathi, B.; et al. Evaluation of Hydroxyapatite Nanoparticles−Induced *in vivo* Toxicity in *Drosophila melanogaster*. *Appl. Surf. Sci.* **2019**, *484*, 568−577.
(70) Basso, A.; Sonvico, A. Identification and in situ Hybridization to Mitotic Chromosomes of A Molecular Marker Linked to Maleness in *Anastrepha fraterculus* (Wied.). *J. Appl. Biotechnol. Bioeng.* **2020**, *7*, 237−240.
(71) Kang, D.; Liu, G.; Gunne, H.; Steiner, H. PCR Differential Display of Immune Gene Expression in *Trichoplusiani*. *Insect Biochem. Mol. Biol.* **1996**, *26*, 177−184.
(72) Seufi, A. M.; Hafez, E. E.; Galal, F. H. Identification, Phylogenetic Analysis and Expression Profile of an Anionic Insect Defense in Gene, with Antibacterial Activity, From Bacterial-Challenged Cotton Leafworm *Spodoptera littoralis*. *BMC Mol. Biol.* **2011**, *12*, 47.
(73) Nowicki, P.; Kuczer, M.; Schroeder, G.; Czarniewska, E. Disruption of Insect Immunity Using Analogs of the Pleiotropic Insect Peptide Hormone Neb-colloostatin: Nanotech Approach for Pest Control II. *Sci. Rep.* **2021**, *11*, 9459.
(74) Shahzad, K.; Manzoor, F. Nanoformulations and Their Mode of Action in Insects: A Review of Biological Interactions. *Drug Chem. Toxicol.* **2021**, *44*, 1−11.
(75) Dinarello, C. A.; Novick, D.; Kim, S.; Kaplanski, G. Interleukin-18 and IL-18 Binding Protein. *Front. Immunol.* **2013**, *4*, 289.
(76) Bankers-Fulbright, J. L.; Kalli, K. R.; McKean, D. J. Interleukin-1 Signal Transduction. *Life Sci.* **1996**, *59*, 61−83.
(77) March, C. J.; Mosley, B.; Larsen, A.; Cerretti, D. P.; Braedt, G.; Price, V.; Gillis, S.; Henney, C. S.; Kronheim, S. R.; et al. Cloning, Sequence and Expression of Two Distinct Human Interleukin-1 Complementary DNAs. *Nature* **1985**, *315*, 641−647.
(78) Gallagher, G. Interleukin-19: Multiple Roles in Immune Regulation and Disease. *Cytokine Growth Factor Rev.* **2010**, *21*, 345−352.

https://doi.org/10.1021/acsomega.3c06134
ACS Omega 2023, 8, 44867−44879